Orbitally forced ice sheet fluctuations during the Marinoan Snowball Earth glaciation

Benn, Douglas I.; Le Hir, Guillaume; Bao, Huiming; Donnadieu, Yannick; Dumas, Christophe; Fleming, Edward J.; Hambrey, Michael J.; McMillan, Emily A.; Petronis, Michael S.; Ramstein, Gilles; Stevenson, Carl T. E.; Wynn, Peter M.; Fairchild, Ian J.

Document Version
Peer reviewed version

Orbitally Forced Ice Sheet Fluctuations in Snowball Earth

Douglas I. Benn,[1,2*] Guillaume Le Hir,[3] Huiming Bao,[4] Yannick Donnadieu,[5] Christophe

Dumas,[5] Edward J. Fleming,[1,6,7] Michael J. Hambrey,[8] Emily A. McMillan,[6] Michael S.

Petronis,[9] Gilles Ramstein,[5] Carl T.E. Stevenson,[6] Peter M. Wynn,[10] Ian J. Fairchild[6]

_____

[1]Department of Geology, The University Centre in Svalbard (UNIS), N-9171 Longyearbyen, Norway.

[2]School of Geography and Geosciences, University of St Andrews, St Andrews KY16 8YA, Scotland, UK.

[3]Institut de Physique du Globe de Paris, Paris, France

[4] Department of Geology and Geophysics, E235 Howe-Russell Complex, Louisiana State University,

    Baton Rouge, LA 70803, USA.

[5]Laboratoire des Sciences du Climat et de l'Environnement, CNRS-CEA, Gif-sur-Yvette, France

[6]School of Geography, Earth and Environmental Sciences, University of Birmingham B15 2TT, UK.

[7]Current address: CASP, West Building, 181A Huntingdon Road, Cambridge, CB3 0DH, UK

[8]Institute of Geography and Earth Sciences, Aberystwyth University, Aberystwyth, Wales, UK.

[9] Natural Resource Management, Environmental Geology,, New Mexico Highlands University,

Las Vegas, New Mexico, USA.

[10]Lancaster Environment Centre, University of Lancaster, Lancaster LA1 4YQ, UK.

*Corresponding author. E-mail: Doug.Benn@unis.no

Snowball Earth theory provides a powerful framework for understanding Neoproterozoic panglaciations, although some of its predictions are apparently contradicted by geological evidence. For example, Snowball theory posits that the panglaciations were terminated after millions of years of frigidity by a positive feedback, in which initial warming from rising atmospheric CO$_2$ was amplified by reduction of ice cover and planetary albedo (1, 2). This threshold behaviour implies that most of the glacial record was deposited in a brief 'melt-back' period (3), an interpretation apparently inconsistent with geological evidence for glacial-interglacial cycles in low palaeolatitudes (4-6). <u>Here w</u>~~W~~e use geological and geochemical evidence combined with numerical modeling experiments to reconcile these apparently conflicting views. New evidence from Svalbard (Norwegian High Arctic) indicates oscillating glacier extent and hydrological conditions within continental deposits of a Cryogenian glaciation, during a period when pCO$_2$ was uniformly high. Modeling experiments show that such oscillations can be explained by orbital forcing in the late stages of a 'Snowball' glaciation, while pCO$_2$ was rising towards the threshold required for complete melt-back. <u>This reconciles Snowball Earth theory with evidence for the complex successions observed at many other localities.</u>

The Wilsonbreen Formation in NE Svalbard contains a detailed record of environmental change during the Marinoan, the second of the major Cryogenian glaciations (650-635 Ma) (7, 8). At this time, Svalbard was located in the Tropics on the eastern side of Rodinia (9, 10). The Wilsonbreen Formation is up to up to 180 m thick and was deposited within a long-lived intracratonic sedimentary basin (11). It is subdivided into three members (W1, W2 and W3) based on the relative abundance

25 of diamictite and carbonate beds (7, 8; Fig. 1; Supplementary Figures 1 & 2). The

26 occurrence of lacustrine sediments containing both precipitated carbonate and

27 ice-rafted detritus throughout the succession, and intermittent evaporative

28 carbonates and fluvial deposits, indicates ~~deposition in a closed terrestrial basin.~~

29 ~~T~~that ~~t~~he basin remained isolated from the sea throughout deposition of the

30 Wilsonbreen Formation, consistent with ~~due to~~ eustatic sea level fall of several

31 hundred metres ~~during the Marinoan~~and limited local isostatic depression

32 (Supplementary Information; 12). This makes it an ideal location to investigate the

33 possibility of climate cycles within a Neoproterozoic panglaciation, as it provides

34 direct evidence of subaerial environments and climatic conditions.

35 　We made detailed sedimentary logs at ten known and new localities extending

36 over 60 km of strike (Fig. 1; Supplementary Figure 1; see Methods). Seven sediment

37 facies associations were identified, recording distinct depositional environments that

38 varied in spatial extent through time (Supplementary Figure 3; Supplementary

39 Information). These are: FA1: *Subglacial*, recording direct presence of glacier ice,

40 FA2: *Fluvial channels*, FA3: *Dolomitic floodplain*, recording episodic flooding,

41 evaporation and microbial communities; FA4: *Carbonate lake margin*, including

42 evidence of wave action; FA5: *Carbonate lacustrine*, including annual rhythmites and

43 intermittent ice-rafted debris; FA6: *Glacilacustrine*, consisting of ice-proximal

44 grounding-line fans (FA6-G) and ice-distal rainout deposits (FA6-D); and FA7:

45 *Periglacial,* recording cold, non-glacial conditions. Additional descriptions are

46 provided in the Supplementary Information. The vertical and horizontal distribution

47 of these facies associations (Fig. 1) allows the sequence of environmental changes to

48 be reconstructed in detail.

49   (1) The base of the Formation is a well-marked periglacially weathered horizon

50   with thin wind-blown sands (Supplementary Figure 4a-b). This surface records very

51   limited sediment cycling in cold, arid conditions.

52   (2) At all localities, the weathering horizon is overlain by fluvial channel facies

53   (FA2) and mudstones, marking the appearance of flowing water in the basin and

54   implying positive air temperatures for at least part of the time (Supplementary

55   Figure 5a).

56   (3) Glacilacustrine deposits (FA6-D) record flooding of the basin and delivery of

57   sediment by ice-rafting (Supplementary Figure 4c-d). Far-travelled clasts are

58   common, indicating transport by a large, continental ice sheet.

59   (4) Warm-based, active ice advanced into the basin, indicated by traction tills and

60   glacitectonic shearing (FA1; Supplementary Figure 4e-g).

61   (5) Ice retreat is recorded by a second periglacial weathering surface (FA7)

62   developed on unconsolidated sediment at the top of member W1. This is overlain by

63   fluvial channel, floodplain, lake-margin and carbonate lacustrine sediments of W2

64   (FA2-5; Supplementary Figure 5), recording a shifting mosaic of playa lakes and

65   ephemeral streams. Lakes and river channels supported microbial communities.

66   Millimetre-scale carbonate-siliciclastic rhythmites indicate seasonal cycles of

67   photosynthesis. Overall, the environment appears to have been closely similar to

68   that of the present-day McMurdo Dry Valleys in Antarctica, though with less extreme

69   seasonality due to its low latitude (13).

70   (6) Water levels and glacier extent underwent a series of oscillations, recorded by

71   switches between glacilacustrine diamictite (FA6-D) and fluvial, lacustrine and lake-

72   margin sediments (FA2-5) in member W2. Sedimentation rates inferred from annual

73 rhythmites in member W2 suggest that each retreat phase may have lasted ~10^4

74 years.

75   (7) A second major ice advance marks the base of W3, with widespread

76 deposition of subglacial tills and glacitectonism of underlying sediments. Basal tills

77 are absent from the northernmost locality, but close proximity of glacier ice is

78 recorded by grounding-line fans (FA6-G; Supplementary Figure 4h-i).

79   (8) Ice retreated while the basin remained flooded and glacigenic sediment

80 continued to be delivered to the lake by ice rafting. Thin laminated carbonates (FA5)

81 in W3 indicate periods of reduced glacigenic sedimentation, indicative of minor

82 climatic fluctuations over timescales of ~10^3 years (Supplementary Figure 5g).

83   (9) A sharp contact with overlying laminated 'cap' carbonate (Supplementary

84 Figure 2) records the transition to post-glacial conditions. At some localities, basal

85 conglomerates provide evidence of subaerial exposure followed by marine

86 transgression. The cap carbonate closely resembles basal Ediacaran carbonates

87 elsewhere, and marks global deglaciation, eustatic sea-level rise and connection of

88 the basin to the sea (1, 12, 14).

89   Environmental and atmospheric conditions during deposition of W2 and W3 can

90 be further elucidated by isotopic data from carbonate-associated sulphate in

91 lacustrine limestones (Fig. 2 and Supplementary Figure 6). These display negative to

92 extremely negative $\Delta^{17}O$ values with consistent linear co-variation with $\delta^{34}S$,

93 indicating mixing of pre-glacial sulphate and isotopically light sulphate formed in a

94 CO_2-enriched atmosphere (15, 16). The observed values could reflect non-unique

95 combinations of $p\mathrm{CO_2}$, $p\mathrm{O_2}$, O_2 residence time and other factors, but a box model

96 (17) indicates $p\mathrm{CO_2}$ was most likely ~10 to 100 mbar (1 mbar = 1000 ppmv).

97   These values are too high to allow formation of low-latitude ice sheets in the

98   Neoproterozoic, but they are consistent with a late-stage Snowball Earth. For an ice-

99   free Neoproterozoic Earth, model studies indicate mean terrestrial temperatures in

100   the range 30-50°C for pCO$_2$ = 10 to 100 mbar (18). Formation of low-latitude ice

101   sheets requires much lower pCO$_2$, on the order of 0.1 - 1 mbar (2, 19, 20), but once

102   formed, high albedo ice cover can maintain low planetary temperatures despite

103   rising pCO$_2$. This hysteresis in the relationship between pCO$_2$ and planetary

104   temperature is a key element of Snowball Earth theory. It implies that W2 and W3

105   were deposited relatively late in the Marinoan, after volcanic outgassing had raised

106   pCO$_2$ from 0.1 or 1 mbar to 10 or 100 mbar. Modelled silicate weathering and

107   volcanic outgassing rates indicate that this would require 10^6 to 10^7 years (21).

108   The consistent co-variation of Δ^{17}O and δ^{34}S in lacustrine limestones in both W2

109   and W3 suggests no detectable rise in atmospheric pCO$_2$, as this would alter the

110   slope of the mixing line (Fig. 2). This implies that the glacier oscillations recorded

111   in~~deposition of both~~ W2 and W3 occurred ~~in~~ during a relatively short time interval

112   (<10^5 years, 21)~~. We therefore infer that the glacier oscillations recorded in the~~

113   ~~Wilsonbreen Formation occurred during a relatively brief period~~ toward the end of

114   the Marinoan.~~ , whereas the much longer period during which~~This implies a long

115   hiatus in the geological record, while pCO$_2$ built up from the low values necessary to

116   initiate low-latitude glaciation (0.1 ~~or~~ to 1 mbar) to those indicated by the

117   geochemical evidence. ~~may have been characterized by cold, arid conditions~~

118   ~~represented only by t~~The basal weathering horizon may record cold arid conditions

119   during part of this interval.

120   The evidence for ice-sheet advance/retreat cycles at low latitudes in a CO_2-

121   enriched atmosphere motivated a series of numerical simulations to test the

122   hypothesis that these cycles were linked to Milankovitch orbital variations. We

123   employed asynchronous coupling of a 3D ice sheet model and an Atmospheric

124   General Circulation Model using the continental configuration of (22). We first ran

125   simulations with a modern orbital configuration to examine ice-sheet behaviour

126   through a large range of pCO$_2$ values from 0.1 to 100 mbar, as used in previous

127   studies (23; Supplementary Figures 7-10). Consistently with previous results (2, 20),

128   at low pCO$_2$ (0.1 mbar), global ice volume reaches 170 x 10^6 km^3 but substantial

129   tropical land areas remain ice free due to sublimation exceeding snowfall

130   (Supplementary Figure S10a). Ice volume remains relatively constant for pCO$_2$ = 0.1

131   to 20 mbar (Supplementary Figure S10b), due to an increase in accumulation that

132   compensates for higher ablation rates (Supplementary Figure 13). In contrast, above

133   20 mbar, ice extent in the eastern Tropics significantly decreases (Supplementary

134   Figure 10c). At pCO$_2$ = 100 mbar, most of the continental ice cover disappears except

135   for remnants over mountain ranges (Supplementary Figure 10d).

136   To test the sensitivity of the tropical ice sheets to Milankovitch forcing,

137   experiments with changing orbital parameters were initialized using the steady-state

138   ice sheets for pCO$_2$ = 20 mbar. Although obliquity has been invoked as a possible

139   cause of Neoproterozoic glaciations (24), this mechanism remains problematical and

140   cannot account for significant climatic oscillations at low latitudes (25, 26). We

141   therefore focused on precession as a possible driver, and used two opposite orbital

142   configurations favoring cold and warm summers, respectively, over the northern

143   tropics (CSO: cold summer orbit and WSO: warm summer orbit) (Supplementary

144 Figure 14). Switching between these configurations causes tropical ice-sheets to

145 advance/retreat over several hundred kilometers in 10 kyr (Supplementary Movie 1),

146 with strong asymmetry between hemispheres (Fig. 3). Shifting from WSO to CSO

147 causes ice retreat in the southern hemisphere, while ice sheet expansion occurs in

148 the northern hemisphere (Supplementary Figure 14c-d). Significant ice volume

149 changes occur between 30° N and S, but are less apparent in higher latitudes. This

150 reflects higher ablation rates in the warmer low latitudes (Supplementary Figure

151 14e-h), and higher ice-sheet sensitivity to shifting patterns of melt. Larger

152 greenhouse forcing at the end of the Snowball event implies increasing ice-sheet

153 sensitivity to subtle insolation changes. Given a strong diurnal cycle (23), our

154 simulations also predict a significant number of days above 0°C in the tropics

155 (Supplementary Figure 15), consistent with geological evidence for ice rafting, liquid

156 water in lakes and rivers, and photosynthetic microbial communities.

157 Our results show that geological evidence for glacial-interglacial cycles (5-7) is

158 consistent with an enriched Snowball Earth theory. Termination of the Marinoan

159 panglaciation was not a simple switch from icehouse to greenhouse states but was

160 characterized by a climate transition during which glacial cycles could be forced by

161 Milankovitch orbital variations. The geochemical evidence presented here implies

162 that at least the upper 60-70% of the Wilsonbreen Formation was deposited in ~10^5

163 years, on the assumption that a trend in pCO$_2$ would be evident over longer

164 timescales (21). Rates of CO$_2$ build-up, however, may have significantly slowed in the

165 later stages of Snowball Earth due to silicate weathering of exposed land surfaces, so

166 it is possible that the oscillatory phase was more prolonged.

167 ~~The~~ Initiation of low latitude glaciation in the Neoproterozoic requires low pCO$_2$

168 (0.1 - 1 mbar, 2, 19, 20), implying that the oscillatory phase was preceded by a

169 prolonged period (~10^6 to 10^7 years) during which pCO$_2$ gradually increased by

170 volcanic outgassing (21) ~~from the low levels (0.1 - 1 mbar) required for glacial~~

171 ~~initiation.~~ ~~In the Wilsonbreen Formation, this period appears to be represented~~

172 ~~solely by the basal weathering horizon, consistent with a 'deep Snowball' state with~~

173 ~~low temperatures and a limited hydrological cycle.~~ This timescale is consistent with

174 recent dating evidence for the duration of Cryogenian glaciations (27).

175 Additional work is needed to refine the upper and lower limits of pCO$_2$ conducive

176 to climate and ice-sheet oscillations in Snowball Earth. Factors not included in the

177 present model, such as supraglacial dust or areas of ice-free tropical ocean (28-30),

178 can be expected to make the Earth system more sensitive to orbital forcing. While

179 many details remain to be investigated, our overall conclusions remain robust.

180 The Neoproterozoic Snowball Earth was nuanced, varied and rich. We anticipate

181 that detailed studies of the rock record in other parts of the world, in conjunction

182 with numerical modeling studies, will continue to yield insight into the temporal and

183 regional diversity of this pivotal period in Earth history.

184

185

186 **Methods**

187

188 **Sedimentology.** Lithofacies were classified based on grain size, internal sedimentary

189 structures and deformation structures, and bounding surfaces. Detailed stratigraphic

190 logs were made in the field, supplemented by drawings and photographs of key

191   features. Samples were taken for polishing and thin sectioning, to allow detailed

192   examination of microstructures in the laboratory. In addition, data were collected on

193   clast lithology, shape, surface features and fabric. Diamictites of the Wilsonbreen

194   Formation are commonly very friable, allowing included clasts to be removed intact

195   from the surrounding matrix, allowing measurement of both clast morphology and

196   orientation, using methods developed for unlithified sediments. Clast morphology

197   (shape, roundness and surface texture) was measured for samples of 50 clasts to

198   determine transport pathways. Clast fabric analysis was performed by measuring a-

199   axis orientations of samples of 50 clasts with a compass-clinometer, and data were

200   summarized using the eigenvalue or orientation tensor method. Orientated samples

201   for measurement of Anisotropy of Magnetic Susceptibility (AMS) were collected

202   using a combination of field-drilling and block sampling. AMS was measured using an

203   AGICO KLY-3 Kappabridge operating at 875 Hz with a 300 A/m applied field at the

204   University of Birmingham and an AGICO MFK-1A Kappabridge operating at 976 Hz

205   with a 200 A/m applied field at New Mexico Highlands University.

206

207   **Geochemistry.** Laboratory procedures for extracting, purifying, and measuring the

208   triple oxygen ($\delta^{18}O$ and $\Delta^{17}O$) and sulfur ($\delta^{34}S$) isotope composition of CAS in bulk

209   carbonates are detailed in ref 16. Briefly, fresh carbonate-bearing rock chips were

210   crushed into fine grains and powders using mortar and pestle. Rinsing the fines with

211   18 MΩ water revealed little water-leachable sulphate in all the Wilsonbreen

212   carbonates. Subsequently, ca. 10 to 30 g carbonates were slowly digested in 1-3 M

213   HCl solutions. The solution was then centrifuged, filtered through a 0.2 μm filter, and

214   acidified before saturated $BaCl_2$ droplets were added. $BaSO_4$ precipitates were

215   collected after >12 hours and purified using the DDARP method (see Supporting

216   Information). The purified $BaSO_4$ was then analyzed for three different isotope

217   parameters: 1) $\Delta^{17}O$, by converting to O_2 using a CO_2-laser fluorination method; 2)

218    $\delta^{18}O$, by converting to CO through a Thermal Conversion Elemental Analyzer (TCEA)

219   at 1450 °C; and 3) $\delta^{34}S$, by converting to SO_2 by combustion in tin capsules in the

220   presence of V_2O_5 through an Elementar Pyrocube elemental analyzer at 1050 °C. The

221    $\Delta^{17}O$ was run in dual-inlet mode while the $\delta^{18}O$ and $\delta^{34}S$ in continuous-flow mode.

222   Both the $\Delta^{17}O$ and $\delta^{18}O$ were run on a MAT 253 at Louisiana State University whilst

223   the $\delta^{34}S$ was determined on an Isoprime 100 continuous flow mass spectrometer at

224   the University of Lancaster, UK. The $\Delta^{17}O$ was calculated as $\Delta^{17}O \equiv \delta'^{17}O - 0.52 \times \delta'^{18}O$

225   in which $\delta' \equiv 1000\ln(R_{sample}/R_{standard})$ and R is the molar ratio of $^{18}O/^{16}O$ or $^{17}O/^{16}O$.

226   All δ values are in VSMOW and VCDT for sulphate oxygen and sulfur respectively.

227   The analytical standard deviation (1σ) for replicate analysis associated with the $\Delta^{17}O$,

228    $\delta^{18}O$, and $\delta^{34}S$ are ±0.05‰, ±0.5‰, and ±0.2‰, respectively. Since the CAS is

229   heterogeneous in hand-specimen, the standard deviation is for laboratory

230   procedures. $\delta^{34}S$ values were corrected against VCDT using within run analyses of

231   international standard NBS-127 (assuming $\delta^{34}S$ values of +21.1 ‰). Within-run

232   standard replication (1 SD) was <0.3 ‰. All geochemical data are included in

233   Supplementary Table 1.

234

235   Details of the numerical modelling are provided in the Supplementary Information in

236   the online version of the paper. Code for the GCM LMDz is freely available at:

237   http://lmdz.lmd.jussieu.fr but the ISM GRISLI (GRenoble Ice Shelf and Land Ice

238   model) is in limited access.
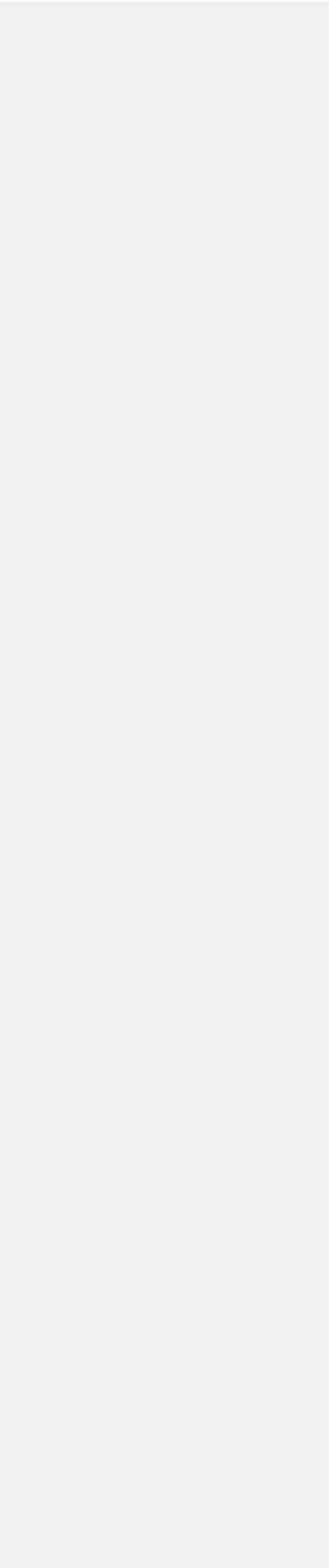
References

(1) Hoffman, P.F. and Schrag, D.P. The Snowball Earth hypothesis: testing the limits of global change. *Terra Nova* **14**, 129-155 (2002).

(2) Donnadieu, Y., Goddéris, Y. and Le Hir, G. Neoproterozoic atmospheres and glaciation. In: *Treatise on Geochemistry*, Second Edition Vol. 6, 217-229 (2014).

(3) Hoffman, P.F. Strange bedfellows: glacial diamictite and cap carbonate from the Marinoan (635Ma) glaciation in Namibia. *Sedimentology* **58**, 57-119 (2011).

(4) Allen, P.A. and Etienne, J.L. Sedimentary challenge to Snowball Earth. *Nat Geosci* **1**, 817-825 (2008).

(5) Rieu, R., Allen, P.A., Plötze, M. and Pettke, T. Climatic cycles during a Neoproterozoic "snowball' glacial epoch. *Geology* **35**, 299-302 (2007).

(6) Le Heron, D.P., Busfield, M.E., and Kamona, F. An interglacial on snowball Earth? Dynamic ice behaviour revealed in the Chuos Formation, Namibia*. Sedimentology* **60***,* 411-427 (2013).

(7) Fairchild, I.J. and Hambrey, M.J. Vendian basin evolution in East Greenland and NE Svalbard. *Precambrian Res* **73**, 217–233 (1995).

(8) Halverson, G.P. A Neoproterozoic Chronology IN: Xiao, S. & Kaufman, A.J. (Eds.) *Neoproterozoic Geobiology and Paleobiology*, 231-271 (Springer, New York, 2006).

(9) Li, X.-X., Evans, D.A. and Halverson, G.P. Neoproterozoic glaciations in a revised global palaeogeography from the breakup of Rodinia to the assembly of Gondwanaland. *Sediment Geol* **294**, 219-232 (2013).

(10) Petronis, M S, Stevenson, C, Fleming, E J, Fairchild, I J, Hambrey, M, Benn, D I., 2013, Paleomagnetic Data from the Neoproterozoic Wilsonbreen Formation, Ny Friesland, Svalbard, Norway and Preliminary Data from the Storeelv Formation, Ella Ø, Kong Oscar Fjord, East Greenland, American Geophysical Union, Fall Meeting 2013, abstract #GP41A-1107.

(11) Harland, W.B. *The Geology of Svalbard*. Geol. Soc. London Mem., 17 (Geological Society, London, 1997).

(12) Creveling, J.R. and Mitrovica, J.X. The sea-level fingerprint of a Snowball Earth deglaciation. *Earth Planet Sc Lett* **399**, 74–85 (2014).

(13) Lyons, W.B. et al. The McMurdo Dry Valleys long-term ecological research program: new understanding of the biogeochemistry of the Dry Valley lakes: a review. *Polar Geography* **25**, 202-217 (2001).

(14) Hoffman, P. et al. Are basal Ediacaran (635 Ma) basal 'cap dolostones' diachronous? *Earth Planet Sc Lett* **258**, 114-131 (2007).

(15) Fairchild, I.J., Hambrey, M.J., Spiro, B. and Jefferson, T.H. Late Proterozoic glacial carbonates in northeast Spitsbergen: new insights into the carbonate-tillite association. *Geol Mag* **126**, 469-490 (1989).

(16) Bao, H., Fairchild, I.J, Wynn, P.M. and Spötl, C. Stretching the envelope of past surface environments: Neoproterozoic glacial lakes from Svalbard. *Science* **323**,119-122 (2009).

(17) Cao, X. and Bao, H. Dynamic model constraints on oxygen-17 depletion in atmospheric O_2 after a Snowball Earth. P Natl Acad Sci USA **110**, 14546–14550 (2013).

(18) Le Hir, G. et al. The snowball Earth aftermath: Exploring the limits of continental weathering processes. *Earth Planet Sc Lett* **277**, 453–463 (2009).

(19) Pierrehumbert, R., Abbot, D.S., Voigt, A. and Koll, D. Climate of the Neoproterozoic. *Ann Rev Earth Planet Sci* **39**, 417-460 (2011).

(20) Pollard, D. and Kasting, J.F. Climate-ice simulations of Neoproterozoic glaciation before and after collapse to Snowball Earth. In: G.S. Jenkins, M.A.S. McMenamin, C.P. McKay and L. Sohl (eds.) *The Extreme Proterozoic: Geology, Geochemistry, and Climate.* Geophys. Monogr. Ser. 146 (AGU, Washington, D.C. 2004).

(21) Le Hir, G., Ramstein, G., Donnadiieu, Y. and Goddéris, Y. Scenario for the evolution of atmospheric pCO_2 during a snowball Earth. *Geology* **36***, 47–50 (2008)*.

(22) Hoffman, P.F., Li, Z.X., A palaeogeographic context for Neoproterozoic glaciation. *Palaeogeogr Palaeocl* **277**, 158–172 (2009).

(23) Pierrehumbert, R.T. Climate dynamics of a hard Snowball Earth. *J Geophys Res* **110**, DOI: 10.1029/2004JD005162 (2005).

(24) Spiegl, T. C., Paeth, H. and Frimmel, H.E., Evaluating key parameters for the initiation of a Neoproterozoic Snowball Earth with a single Earth System Model of intermediate complexity. *Earth Planet Sc Lett* **415**, 100-110 (2015).

(25) Donnadieu, Y., Ramstein, G., Fluteau, F., Besse, J. and Meert, J. Is high obliquity a plausible cause for Neoproterozoic glaciations? *Geophys Res Lett* **29**, DOI: 10.1029/2002GL015902 (2002).

(26) Paillard, D. Quaternary glaciations: from observations to theories. *Quaternary Sci Rev* **107**, 11-24 (2015).

(27) Rooney, A.D. et al. ~~Re-Os geochronology and coupled Os-Sr isotope constraints on the Sturtian snowball Earth. *PNAS* **111**, doi: 10.1073/pnas.1317266110~~A Cryogenican chronology: Two long-lasting synchronous Neoproterozoic glaciations. Geology 43, 459-462 (2015~~2014~~).

(28) Abbot, D.S. and Pierrehumbert, R.T. Mudball: surface dust and Snowball Earth deglaciation. J Geophys Res **115,** DOI: 10.1029/2009JD012007 (2010).

(29) Abbot, D.S., Voigt, S. and Koll, D. The Jormungand global climate state and implications for Neoproterozoic glaciations. *J Geophys Res-Atmos* 116, DOI: 10.1029/2011JD015927 (2011).

(30) Rose, B. E. J. Stable "Waterbelt" climates controlled by tropical ocean heat transport: A nonlinear coupled climate mechanism of relevance to Snowball Earth. *J Geophys Res-Atmos* **120**, doi:10.1002/2014JD022659 (2015).

Correspondence and requests for materials should be addressed to Doug Benn (doug.benn@unis.no).

Author contributions

Field data were collected and analyzed by IJF, DIB, EJF, MJH, EAMcM, MSP, PMW and CTES. Geochemical analyses were conducted by HB and PMW. Model experiments were designed and conducted by GLeH, YD, CD and GR. The manuscript and figures were drafted by DIB, IJF and GLeH, with contributions from the other authors.

Competing financial interests

The authors declare no competing financial interests.
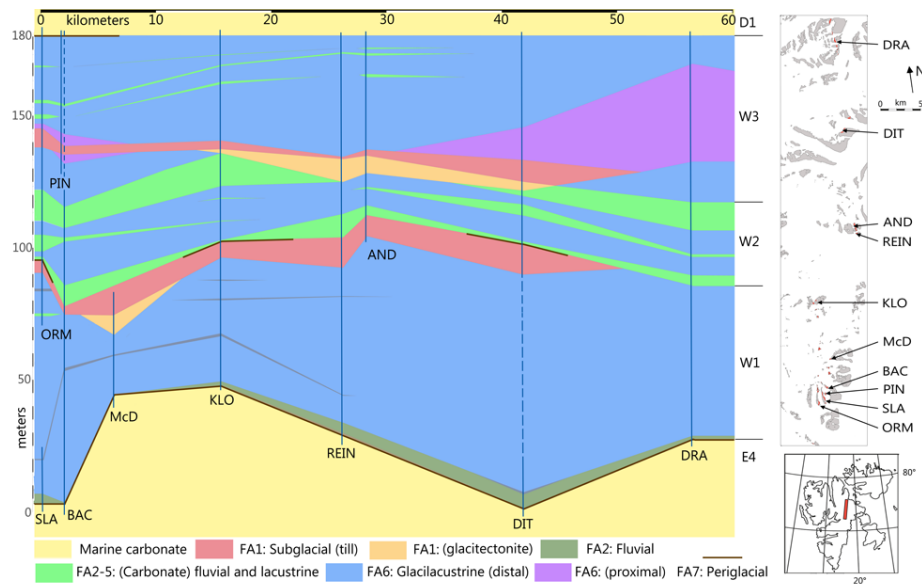
Figures:

Figure 1: Sedimentary architecture and palaeoenvironments of the Wilsonbreen Formation. Regional correlation of facies associations and members W1, W2 and W3 across NE Svalbard. From north to south, study locations are: DRA: Dracoisen; DIT: Ditlovtoppen; AND: East Andromedafjellet; REIN: Reinsryggen (informal name); KLO: Klofjellet; McD: MacDonaldryggen; BAC: Backlundtoppen - Kvitfjellet ridge; PIN: Pinnsvinryggen (informal name); SLA: Slangen and ORM: Ormen.
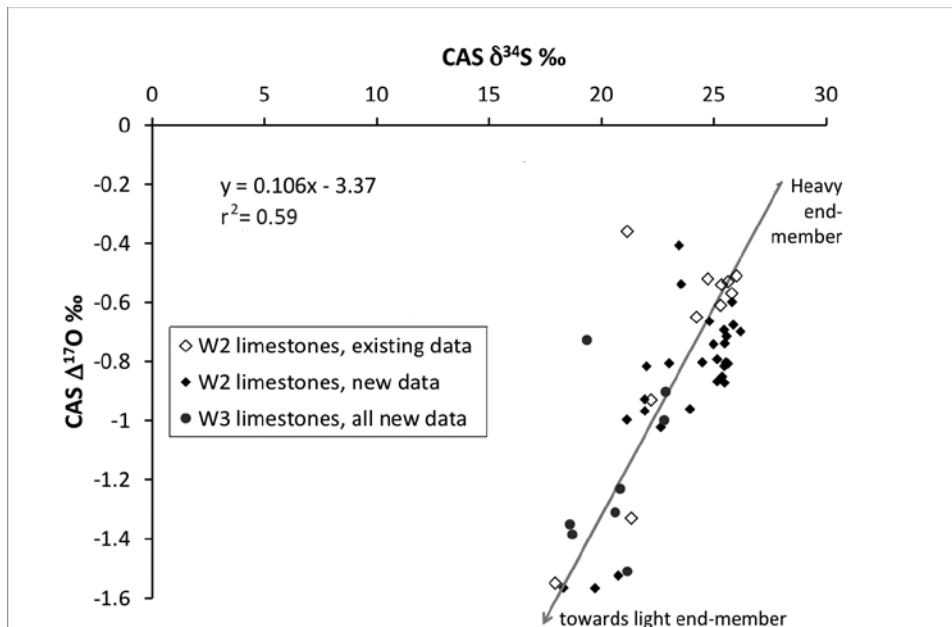
Figure 2: Co-variation of $\Delta^{17}O$ and $\delta^{34}S$ from carbonate-associated sulphate in W2 and W3. 'Existing data' (ref. 16) and new data define a mixing line between pre-glacial sulphate (top) and an isotopically light sulphate formed by oxidation of pyrite including incorporation of a light-$\Delta^{17}O$ signature from a CO_2-enriched atmosphere. Data from W2 and W3 lie on closely similar trend lines, indicating no detectable change in pCO_2 between deposition of the two members.

(a) ice thickness [WSO, 20kyrs of simulation]

(b) ice thickness [CSO, 30kyrs of simulation]
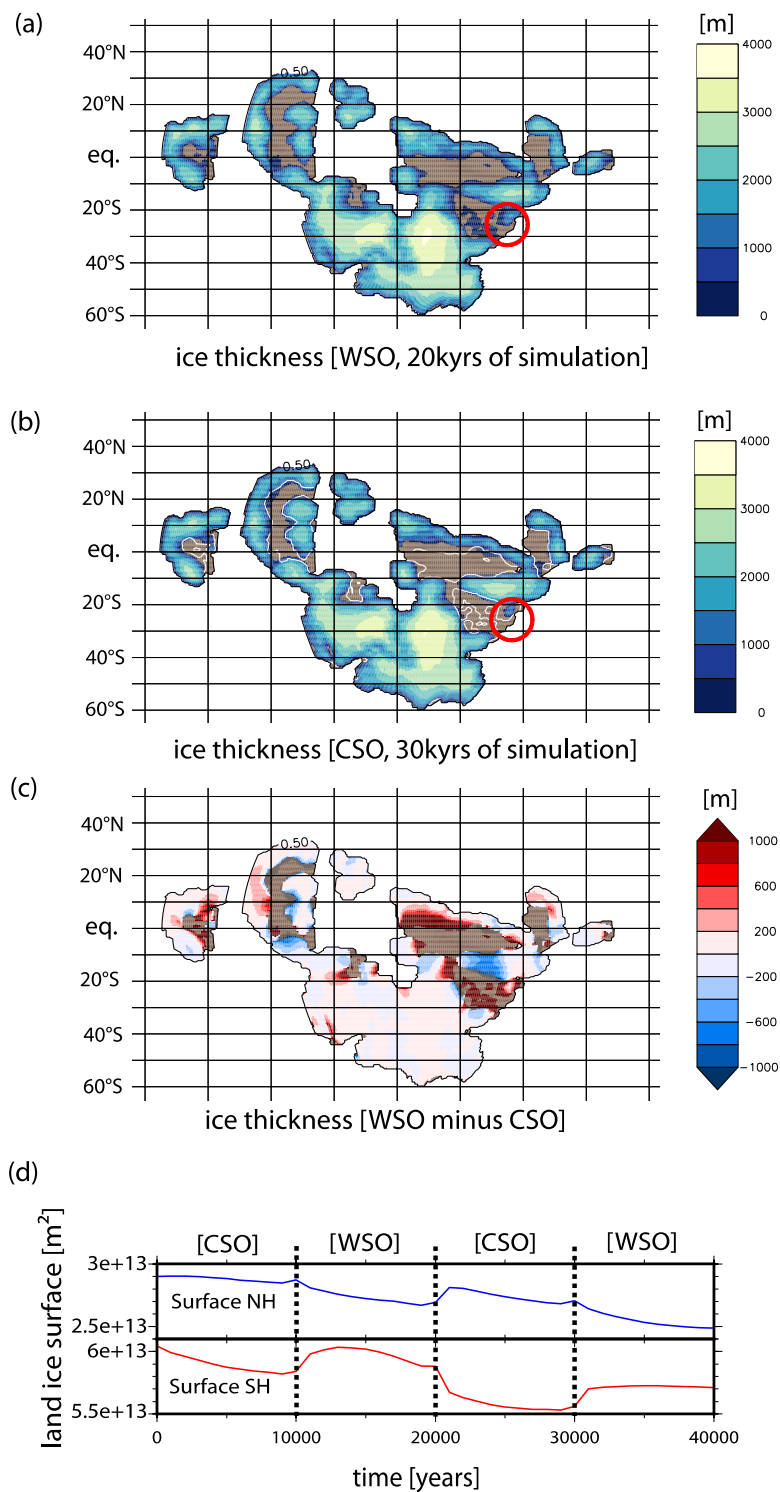
(c) ice thickness [WSO minus CSO]

(d)

Figure 3: Modelled ice sheet oscillations in response to orbital forcing. (a), (b)

shaded contours show land ice thickness obtained with 20 mbar of carbon dioxide in response to changes of orbital forcing (WSO and CSO, warm/cold summer orbit for the northern hemisphere) over the course of two precession cycles (40 ky of simulation). In light brown continental areas without ice, the white line is used to represent the old ice-sheet extension (WSO case). The Svalbard area is indicated by a red circle. (c) ice thickness variation in 10 ky (WSO case after 20 ky minus CSO case after 30 ky of simulation) (d) surface of hemisphere covered by ice (m^2) through time ([WSO] and [CSO] indicate which orbital configuration is used).